Prediction of physical separation of metals from soils contaminated with municipal solid waste ashes and metallurgical residues

Ikbel Mouedhen [a], Lucie Coudert [b], Jean-François Blais [a, *], Guy Mercier [a]

[a] Institut National de la Recherche Scientifique (Centre Eau Terre Environnement), Université du Québec, 490 rue de la Couronne, Québec, QC G1K 9A9, Canada
[b] Institut de recherche en mines et en environnement (Unité de recherche et de service en technologie minérale), Université du Québec en Abitibi-Témiscamingue, 445 boulevard de l'Université, Rouyn-Noranda, QC J9X 5E4, Canada

ARTICLE INFO

ABSTRACT

Environmental legislation is forcing industrialized countries to rehabilitate contaminated lands. Expensive solutions are available to treat soils contaminated by metals (e.g., solidification, stabilization, and landfilling). Physical remediation techniques, which are less expensive, are able to efficiently separate metals from contaminated soils under specific physical conditions. In the current study, densimetric and mineralogical characterization of fractions of soil between 0.25 and 4 mm contaminated by municipal solid waste (MSW) ashes and metallurgical waste was performed. This characterization confirmed the usefulness of the jig and wet shaking table for separating the metal contaminants from the soil. Mineralogical characterization allowed the prediction of treatment efficiencies and potential limits. The jig performance was optimized based on densimetric characterization. Water washing coupled with ferrous material extraction using magnetic separation, and, attrition scrubbing coupled with the jig and wet shaking table, led to a removal yield varying from 42.1% to 83.4% for Ba, Cu, Pb, Sn, and Zn from the fraction of soil >0.25 mm contaminated by MSW ashes. The recovered treated mass varied from 57.1% to 73.4% (by weight). For the fraction of soil >0.25 mm contaminated with metallurgical residues, Cu and Zn removal yields were higher than 57.5%. The recovered treated mass from this soil fraction corresponded to 64.8% (by weight). Depending on the level and leachability of contaminants, the soil fractions <0.25 mm were recommended for appropriate treatments (solidification or stabilization) or for safe disposal via landfills.

© 2019.

1. Introduction

Heavy metals generally refer to a group of toxic compounds, usually used in the industry and in various modern technologies (Khalid et al., 2017). The extent of inorganic pollution in soils of industrialized countries is of serious concern. Sources of metals in soils include municipal solid waste (MSW) ashes and slags generated during extractive metallurgical operations. Bottom and fly ashes are the main by-products of MSW combustion processes (Forteza et al., 2004). The two main categories of slags produced by metal-manufacturing processes are ferrous slags (e.g., iron slag, steel slag, and alloy steel slag) and non-ferrous slags (e.g., copper slag) (Piatak et al., 2015a).

The selection of the most appropriate soil remediation method depends on the concentration and the nature of pollutants to be removed (Mercier et al., 2001). Physical and mineralogical properties of inorganic compounds derived from MSW ashes are mainly controlled by the characteristics of the incineration system, such as the redox at-

mosphere, thermal conditions during incineration, and composition of incinerated MSW (Dong et al., 2015; Horowitz, 1991; Iskandar, 2000). These inorganic compounds derived from metallurgical residues are controlled by different smelting conditions under which the slag is formed such as the fuel source, initial composition of the ore and flux, and type of blast (cold or hot) (Piatak et al., 2012). Moreover, physical and chemical characteristics of soils (e.g., pH, cation exchange capacity, soil mineralogy, and biological conditions) are involved in the evolution of these metals in the soil (Kabata-Pendias, 2011, Kowalski et al., 2017, Piatak et al., 2012, Shen et al., 2003). Soils polluted by MSW ashes and metallurgical residues can show significant concentrations of metals. For instance, Jobin et al. (2016b) quoted up to 1797 mg/kg, 2775 mg/kg, 879 mg/kg, and 2077 mg/kg of Cu, Pb, Sn, and Zn, respectively, in bulk soils contaminated by MSW ashes. In comparison, Bisone et al. (2013) reported up to 2500 mg/kg of Cu and up to 2240 mg/kg of Zn in bulk soils contaminated by metallurgical residues. Such soils require appropriate management to effectively remove inorganic contaminants and enable a second use of the treated medium.

Physical separation is a non-destructive technique, generally associated with the ore-processing industry. It aims to concentrate metals into a small volume through processes such as particle size separation, attrition scrubbing, magnetic separation, and gravimetric separation. A strong magnetic susceptibility of pollutants or a high liber-

* Corresponding author.
Email addresses: ikbel.mouedhen@ete.inrs.ca (I. Mouedhen); lucie.coudert@uqat.ca (L. Coudert); blaisjf@ete.inrs.ca (J-F Blais); guy.mercier@ete.inrs.ca (G. Mercier)

Table 1
Relative ease of separating minerals using gravity techniques.

Concentration criterion	Separation	Minimum size of particles (μm)[a]
2.5	Relatively easy	75
1.75–2.5	Possible	150
1.5–1.75	Difficult	2000
1.25–1.5	Very difficult	6500
<1.25	Not possible	

[a] Minimum size of particles = Below the indicated value, gravimetric separation is not possible for the corresponding concentration criterion.

ation degree of the mineralogical phase containing heavy metals is often sought to ensure satisfactory efficiency of heavy metal removal (Dermont et al., 2008). Physical treatment (costing 70–187 USD per m^3 of soil) represents a cost-effective and proactive alternative to solidification and stabilization (116–248 USD per m^3 of soil), landfilling (300–510 USD per t of soil), and acid leaching (358–1717 USD per t of soil) treatments (FRTR, 2016c). As a type of physical separation method, a shaking table test enables the treatment of a wide range of particle sizes (0.100–3 mm). The effective treatment of particles with a size of 0.063 mm was also reported using a shaking table for the rehabilitation of sites contaminated by MSW ashes (Mercier et al., 2002, Wills, 2011).

Wet shaking table tests show good potential in isolating inorganic contaminants from soils contaminated via various sources. For instance, treating soils contaminated with weapon ammunition using a shaking table removed up to 96% of Pb (Laporte-Saumure et al., 2010). A wet shaking table effectively removed 26% of Cu when treating a soil contaminated with mining residues (Veetil et al., 2014). For a soil contaminated with slags and smelter residues, a gravimetric device removed up to 68% of Cu. Previous studies on

soils polluted with MSW ashes reported Pb removal yields of 61–80% (Jobin et al., 2015, Mercier et al., 2001). The separation process used in a wet shaking table is generally optimized through numerous randomized trials, increasing treatment costs and rehabilitation time (Bisone et al., 2013, Laporte-Saumure et al., 2010, Veetil et al., 2014). On the other hand, a jig is a gravimetric device frequently used to handle coarse materials with a particle size ranging from 3 to 10 mm. By means of a pulsating water current, a bed of particles is intermittently fluidized and compacted. The harmonic wave causes the stratification of particles in layers with increasing density from the top to bottom. Heavy particles are thereby separated. The main mechanisms involved are differential acceleration, hindered settling, and interstitial trickling (Wills, 2011). As in the case of a wet shaking table, a jig is generally randomly optimized to produce effective results. In the case of soil fractions between 0.5 to 3 mm and 1 to 4 mm sampled from an arm firing range, removal yields for Pb, Cu, Sb, and Zn using a jig were up to 94% (Laporte-Saumure et al., 2010). Jigs have been used for treating soil fractions between 2 to 4 mm and 0.85 to 2 mm contaminated with ashes from MSW incinerators. Removal yields ranged from 47%–67%, 39%–89%, 27%–74%, and 17%–53.7% for Pb, Cu, Sn, and Zn, respectively (Jobin et al., 2015, Mercier et al., 2002).

As mentioned above, the development and optimization of a process train—including physical treatments (e.g., using a shaking table or jig)—usually require numerous randomized trials, increasing both treatment costs and rehabilitation time. Previous papers have mentioned the helpfulness of numerous analysis tools in the choice of decontamination processes and for the establishment of relevant strategies for the rehabilitation of contaminated sites. In fact, microscopic examination of contaminated particles coupled with energy dispersive spectrometry can provide substantial information about the dimension, surface characteristics, and composition of both the pol-
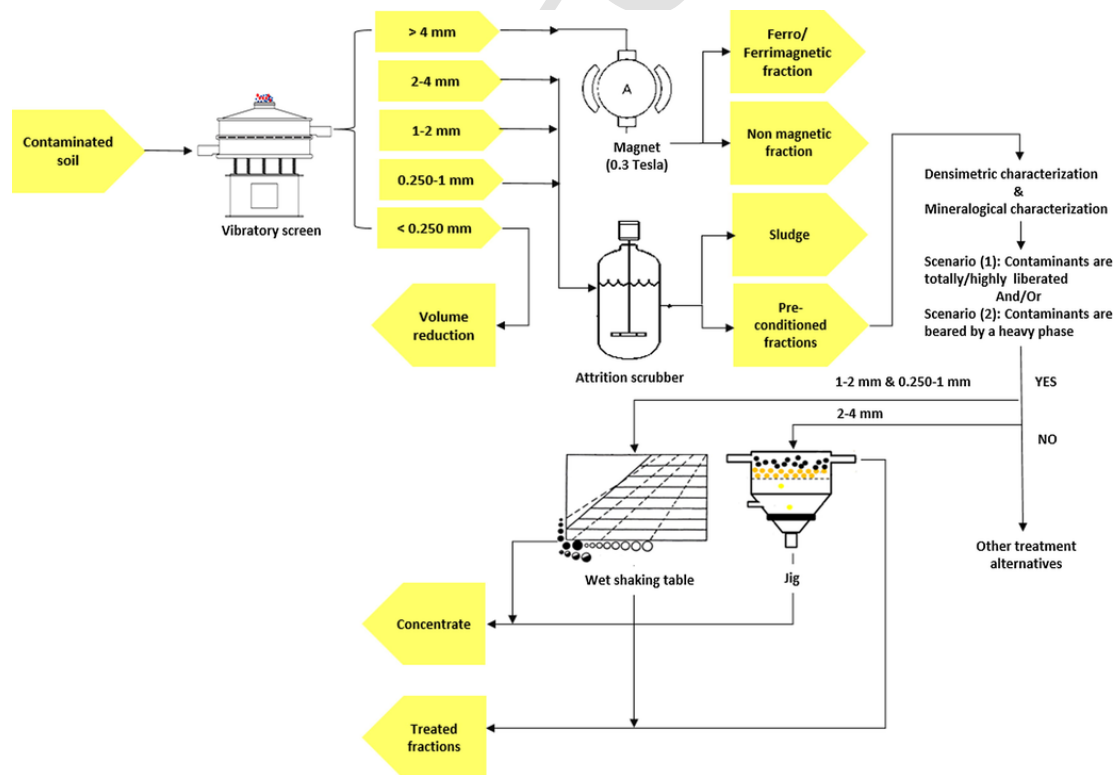

Fig. 1. The proposed physical treatment process.

Table 2
Partitioning of inorganic contaminants present in different particle size fractions of MSW1, MSW2, MSW3 and MR1.

Soil	Soil faction	Mass	Inorganic contaminants										
			Ba		Cu		Pb		Sn		Zn	
	(mm)	(%)	(mg/kg)	(%)	(mg/kg)	(%)	(mg/kg)	(%)	(mg/kg)	(%)	(mg/kg)	(%)
MSW1	>12	22.4	406	16.5	108	7.05	246	6.45	46.9	5.28	969	23.3
	4–12	19.4	375	13.2	513	29.2	491	11.2	177	17.4	677	14.1
	2–4	11.0	489	9.77	589	19.0	783	10.1	284	15.7	935	11.0
	1–2	7.00	529	6.74	458	9.40	1210	9.96	332	11.7	953	7.16
	0.250–1	17.0	324	10.0	183	9.13	942	18.8	175	15.0	514	9.38
	<0.250	23.2	1040	43.7	385	26.2	1600	43.5	299	34.9	1410	35.0
	Total	**100**	**550**	**100**	**341**	**100**	**852**	**100**	**199**	**100**	**932**	**100**
MSW2	>12	31.0	262	14.2	474	25.8	396	11.36	225	16.8	593	15.4
	4–12	15.1	430	11.3	279	7.40	616	8.60	191	6.95	917	11.6
	2–4	10.9	726	13.8	918	17.6	1740	17.5	474	12.4	1360	12.3
	1–2	7.10	643	7.97	727	9.10	1640	10.77	596	10.2	1290	7.65
	0.250–1	16.0	445	12.4	463	13.0	1660	24.6	628	24.2	1200	16.0
	<0.250	19.8	1160	40.3	778	27.1	1480	27.1	620	29.5	2240	37.1
	Total	**100**	**572**	**100**	**569**	**100**	**1080**	**100**	**416**	**100**	**1200**	**100**
MSW3	>12	14.7	483	7.05	1290	16.3	688	5.02	289	5.40	470	4.22
	4–12	21.0	699	14.6	1620	29.3	1700	17.8	977	26.2	1340	17.3
	2–4	18.9	700	13.1	1120	18.3	1820	17.1	703	16.9	1440	16.7
	1–2	8.37	1090	9.06	1120	8.12	3030	12.6	1170	12.5	1810	9.30
	0.250–1	19.9	1,05	20.9	702	12.1	2000	19.8	716	18.2	1510	18.5
	<0.250	17.2	2060	35.2	1070	15.9	3240	27.7	950	20.8	3230	34.0
	Total	**100**	**1000**	**100**	**1160**	**100**	**2010**	**100**	**784**	**100**	**1630**	**100**
MR1	>12	20.3	n.a.[a]	n.a.	1570	10.5	n.a.	n.a.	n.a.	n.a.	963	6.37
	4–12	13.8	n.a.	n.a.	2550	11.5	n.a.	n.a.	n.a.	n.a.	3410	15.1
	2–4	22.7	n.a.	n.a.	2940	21.8	n.a.	n.a.	n.a.	n.a.	4850	35.3
	1–2	10.5	n.a.	n.a.	4190	14.4	n.a.	n.a.	n.a.	n.a.	5390	18.2
	0.250–1	14.5	n.a.	n.a.	3300	15.7	n.a.	n.a.	n.a.	n.a.	2100	9.79
	<0.250	18.0	n.a.	n.a.	4430	26.0	n.a.	n.a.	n.a.	n.a.	2640	15.2
	Total	**100**	n.a.	n.a.	**3060**	**100**	n.a.	n.a.	n.a.	n.a.	**3110**	**100**

[a] n.a = Not applicable.

lutant-bearing phase and its carrying phase (Mercier et al., 2001, Mouedhen et al., 2018). Based on exhaustive mineralogical characterization, Pb particles in soil contaminated by MSW ashes were well described and classified based on the corresponding mineralogy of both the Pb-bearing and carrying phases. Moreover, by considering the mean surface ratio of the carrying phase and the Pb-bearing phase, the densities of particles were estimated. This consequently allowed the prediction of an adequate treatment train and the fate of Pb particles when using physical separation processes including magnetic separation, a jig, and Wilfley table (Mercier et al., 2001). In the same context, as shown in Table 1, the concentration criterion indicates the suitability of using gravimetric processes to separate heavy particles from uncontaminated material. This parameter is calculated and defined as follows (Eq. (1)) (USEPA, 1995):

Concentration criterion calculation

$$\textbf{\textit{Concentration criterion}} = \frac{\textit{Density of heavy particle } (g/cm^3) - \textit{Density of fluid } (g/cm^3)}{\textit{Density of light particle } (g/cm^3) - \textit{Density of fluid } (g/cm^3)}$$

The estimation of heavy particle distributions in a soil sample through the use of dense media separation (DMS) using tetrabromoethane (TBE: $C_2H_2Br_4$) establishes the limit of metal removal that can be achieved using gravimetric devices (e.g., shaking tables and jigs). Densimetric characterization has also been exploited to maximize the performance of wet shaking tables in separating metals from soil contaminated with ashes from MSW incinerators

(Mouedhen et al., 2018). Studies have highlighted the usefulness of densimetric characterization coupled with a shaking table mechanism model, using a statistical approach to both predict and optimize the treatment of soil contaminated with inorganic compounds, while minimizing the number of trials (Mouedhen et al., 2018).

In this paper, a mineralogical characterization of Pb, Sn, Cu, and Zn-bearing phases found in the fraction of soil samples >0.25 mm contaminated with MSW incinerator ashes and metallurgical residues was performed in order to predict the fate of different types of contaminated particles in gravimetric devices (i.e., a shaking table and jig). In addition to previous work on the prediction of the performance of wet shaking tables, this study exploits densimetric characterization data to: (i) evaluate the applicability of gravimetric devices; (ii) define the highest limit of separation; and (iii) optimize the performance of the laboratory jig used. Finally, the paper assesses the performance of a proposed complete process train composed of physical treatment to remediate soils with different types and levels of inorganic pollution.

2. Materials and methods

2.1. Sampling sites

Two abandoned industrial sites in the province of Quebec, eastern Canada, were studied. Based on a previous sampling and characterization campaign, these sites were sectioned in three different areas according to the spatial distribution of contaminants. According to the reported data, the first site, situated in Quebec City, was used as a landfill to dispose MSW ashes from 1940 to 1960. The site was also a snow-dumping ground (Mercier et al., 2002). Three soil samples,

Table 3

Mineralogical examination of a mix of contaminated particles derived from the heavy fraction of the 2–4 mm, 1–2 mm and 0.250–1 mm of soils contaminated by MSW ashes (MSW2 and MSW3). N-P=Identifier of the particle examined; P=Phase; ()=% surface; d=density; CC=Concentration criterion calculated according to the Eq. (1), *=Unidentifiable density.

N-P	Elements in P1	d-P1	Elements in P2	d-P2	Elements in P3	d-P3	Mean d	CC
		(g/cm^3)		(g/cm^3)		(g/cm^3)	(g/cm^3)	
2–4 mm								
1	**Pb**, C, O (3.25)	6.58	Fe, C, O (96.8)	3.90			3.99	1.81
2	**Pb**, C, O (12.5)	6.58	Ba, B, S, O, C (87.5)	4.30-*			4.59-*	2.19-*
3	**Pb**, O (70.6)	9.00	**Pb**, O, Sb, Al (29.4)	4.00–9.00			7.53–9.00	3.98–4.88
4	**Pb**, C, O (2.72)	6.60	Ba, P, O, C (10.4)	4.30-*	Ba, S, O, C (86.9)	4.30–4.48	4.36-*	2.04-*
5	**Pb**, **Zn**, Ti, Si, Al, O, Ca, Cr (65.8)	2.90–3.60	Fe, O (34.2)	5.20–5.30			3.69–4.18	1.64–1.94
6	**Pb**, Fe, O (0.63)	5.20–9.00	Fe, Al, O, Na, Mg, Si, Ca (88.3)	2.90–3.60	Al, O (11.1)	4.00	3.04–3.24	1.24–1.36
7	**Pb**, O, Cl (22.2)	5.85–9.00	**Sn**, Fe, O, Al, Si (12.7)	2.90–3.60	Fe, O (65.1)	5.20–5.30	5.05–5.91	2.47–2.99
8	**Sn**, Fe, C, O (9.49)	3.90	Fe, C, O (90.5)	3.90			3.90	1.76
9	**Sn**, Fe, O (4.31)	5.20–6.90	Fe, O, Al (80.0)	4.00–5.30	AL, O (15.7)	4.00	4.05–4.54	1.86–2.16
10	**Cu**, C, O (100)	3.90					3.90	1.76
11	**Cu**, Cl, O (56.0)	3.42–6.50	**Cu**, O, Al (44.0)	4.00–6.50			3.68–6.50	1.63–3.35
12	**Cu**, C, O (5.58)	3.90	Fe, C, O (94.6)	3.90			3.90	1.76
13	**Cu**, Fe, O (17.4)	5.20–6.50	Fe, O (48.0)	5.20–5.30	Si, Ca, O, Mg, Na, Fe, Al (34.6)	2.90–3.60	4.40–4.92	2.08–2.39
1–2 mm								
14	**Pb**, O (100)	9.00					9.00	4.88
15	**Pb**, Sn, O (100)	6.90–9.00					6.90–9.00	3.60–4.88
16	**Pb**, O (100)	9.00					9.00	4.88
17	**Pb**, Fe, Si, O (100)	2.90–3.60					2.90–3.60	1.16–1.59
18	**Pb**, Fe, O (100)	5.20–9.00					5.20–9.00	2.56–4.88
19	**Pb**, Si, O (91.0)	2.90–3.60	**Pb**, Ca, Si, O (8.96)	2.90–3.60			2.90–3.60	1.16–1.59
20	**Pb**, O (57.4)	9.00	**Pb**, **Sn**, O (42.6)	6.90–9.00			8.10–9.00	4.33–4.88
21	**Pb**, Fe, O (1.29)	5.20–9.00	Fe, O (98.7)	5.20			5.20–5.25	2.56–2.59
22	**Pb**, Al, Si, O (2.57)	2.90–3.60	**Pb**, Si, O (14.5)	2.90–3.60	**Pb**, Fe, Ca, O (82.9)	2.90–3.60	2.90–3.60	1.16–1.59
23	**Pb**, O (1.73)	9.00	**Pb**, Fe, P, O (65.5)	*	**Pb**, **Zn**, O (32.8)	5.50–9.00	*	*
24	**Sn**,Fe, O (6.74)	5.20–6.90	Fe, O (93.3)	5.20			5.20–5.31	2.56–2.63
25	**Sn**, Fe (5.78)	7.30–7.90	Fe, O (94.2)	5.20–5.30			5.32–5.45	2.63–2.71
26	**Sn**,Fe, O (0.95)	5.20–6.90	Fe, O (99.1)	5.20–5.30			5.20–5.32	2.56–2.63
27	**Sn**, Br, Fe, O (5.76)	5.20–6.90	Fe, O (94.2)	5.20–5.30			5.20–5.39	2,56–2.68
28	**Sn**,Fe, O (1.73)	5.20–6.90	Fe, O (98.3)	5.20–5.30			5.20–5.33	2.56–2.64
29	**Sn**,Fe, O (2.86)	5.20–6.90	Fe, O (97.1)	5.20–5.30			5.20–5.35	2.56–2.65
30	**Sn**, O (17.2)	6.90	Ca, O (82.8)	3.35			3.96	1.81
31	**Sn**, Fe, O (3.16)	5.20–6.90	Fe, O (96.8)	5.20–5.30			5.20–5.35	2.56–2.65

Table 3 (*Continued*)

N-P	Elements in P1	d-P1 (g/cm^3)	Elements in P2	d-P2 (g/cm^3)	Elements in P3	d-P3 (g/cm^3)	Mean d (g/cm^3)	CC
32	**Sn**,Fe, O (4.80)	5.20–6.90	Fe, O (95.2)	5.20–5.30			5.20–5.38	2.56–2.67
33	**Sn**, Fe, O (17.7)	5.20–6.90	Fe, O (82.3)	5.20–5.30			5.20–5.58	2.56–2.79
34	**Sn**, **Cu**, Ni, Fe, O (19.7)	5.20–6.90	Fe, O (80.3)	5.20–5.30			5.20–5.62	2.56–2.81
35	**Cu**, O (100)	6.10–6.50					6.10–6.50	3.11–3.35
36	**Cu**, O (61.8)	6.10	Fe, **Cu**, O (38.2)	5.20–6.50			5.76–6.25	2.90–3.20
37	**Sn**, **Cu**, O (100)	6.10–6.90					6.10–6.90	3.11–3.60
38	**Sn**, **Cu**, Fe (4.73)	7.30–8.94	**Sn**, Fe, O (9.46)	5.20–6.90	Fe, O (85.8)	5.20–5.30	5.30–5.62	2.62–2.82
39	**Zn**, Ca, Si, O (49.3)	2.90–3.60	Fe, Si, O (50.7)	2.90–3.60			2.90–3.60	1.16–1.59
40	**Zn**, Fe, O (82.7)	5.20–5.50	**Sn**, Fe, O (9.67)	5.20–6.90	Al, Si, O (7.64)	2.90–3.60	5.27–5.49	2.61–2.74
0.250–1 mm								
41	**Pb**, Al, C, O (100)	6.58-*					6.58-*	3.40-*
42	**Pb**, C, O (100)	6.58					6.58	3.40
43	**Pb**, C, O (100)	6.58					6.58	3.40
44	**Pb**, **Sn**, C, O (43.8)	6.58-*	Al, Si, C, O (56.2)	2.90–3.60			4.51-*	2.14-*
45	**Pb**, C, O (18.7)	6.58	**Sn**, C, O (81.3)	*			*	*
46	**Pb**, Sb, C, O (55.8)	6.60-*	O, C, Al, Na (44.2)	*			*	*
47	**Pb**, C, O (25.8)	6.58	**Pb**, **Sn**, C, O (47.2)	6.58	**Sn**, O (27.0)	6.90	6.67	3.46
48	**Pb**, C, O (12.1)	6.58	Fe, C, O (22.9)	3.90	Al, Ca, Si, O (65.0)	2.90–3.60	3.57–4.03	1.57–1.85
49	**Sn**, O (100)	6.90					6.90	3.60
50	**Sn**, Fe (11.3)	7.30	**Sn**, Fe, C, O (88.7)	3.90-*			4.0.28	2.00
51	**Sn**, Fe (6.42)	7.30	Fe, O (93.6)	5.20–5.30			5.33–5.43	2.64–2.70
52	**Sn**, O (40.9)	6.90	Fe, O (59.1)	5.20–5.30			5.90–5.95	2.99–3.02
53	**Sn**, Fe, C, O (9.82)	3.90	Fe, O (90.2)	5.20–5.30			5.07	2.48
54	**Sn**, Fe (0.27)	7.30	Fe, O (99.7)	5.20–5.30			5.21–5.31	2.56–2.63
55	**Sn**, Fe, C, O (12.0)	3.90	Fe, O (68.3)	5.20–5.30	Ca, C, O (19.7)	2.54	4.52–4.59	2.15–2.19

(MSW1, MSW2, and MSW3) were collected from three different areas of this site.

A fourth soil sample (MR1) was collected from the most contaminated section of the second site. This latter, situated in Montreal, was polluted with slags and smelter residues. This site is known to have been an important area of industrial expansion between 1848 and 1939 and had been occupied by metallurgical and steel production industries (GC, 2018).

2.2. Preparation and characterization of contaminated soils

Fig. 1 illustrates the overall treatment process. The feedstock pre-treatment, feedstock characterization, and mineral processing operations are described below.

2.2.1. Feedstock pre-treatment

Prior to characterization and physical treatment, a grid was used to remove the fractions of soil >12 mm and fractions of soil between 4 and 12 mm for the soil samples MSW1, MSW2, MSW3, and MR1. Remediation techniques available to treat these fractions are limited. Larger fractions are generally safely disposed via landfills or treated using a physical separation column, attrition scrubbing process, magnetic separation, or crushing and physical-chemical treatment (Bisone et al., 2013, Jobin et al., 2016a, Veetil et al., 2014). In this study, simple water washing and a low magnetic field were applied. Soils fractions >4 mm were then treated using a magnet to separate the ferro/ferri magnetic fraction from the non-magnetic fraction. For each soil sample, the fraction <4 mm was then wet-sieved using a vibrating separator (Sweco Vibro Energy@ Separator, LS18). The soil fractions of 2–4 mm, 1–2 mm, 0.25–1 mm, and <0.25 mm were

Table 4
Mineralogical examination of contaminated particles derived from the 2–4 mm, 1–2 mm and 0.250–1 mm of soil contaminated by metallurgical residues). N-P = Identifier of the particle examined; P = Phase; () = % surface; d = density; CC = Concentration criterion calculated according to the Eq. (1), * = Unidentifiable density.

N-P	Elements in P1	d-P1	Elements in P2	d-P2	Elements in P3	d-P3	Elements in P4	d-P4	Mean d	CC
		(g/cm^3)		(g/cm^3)		(g/cm^3)		(g/cm^3)	(g/cm^3)	
2–4 mm										
1	**Cu,** S, O, C (1.27)	3.65–3.90	**Zn**, Al, Mg, K, Ca, Ti, Fe, Si, O (98.7)	2.90–3.60					2.91–3.60	1.16–1.59
2	**Cu,** S, O, C (2.10)	3.65–3.90	**Zn**, Mg, Al, K, Ca, Ti, Si, O (97.9)	2.90–3.60					2.89–3.61	1.15–1.59
3	**Cu,** S, O, C (0.52)	3.65–3.90	Fe, Mg, Al, K, Ca, Si, O, C (99.5)	2.90–3.60					2.91–3.60	1.16–1.59
4	**Cu,** C, O (0.42)	3.90	**Zn**, Fe, Ca, K, Al, Mg, Si, O (99.6)	2.90–3.60					2.90–3.60	1.15–1.58
5	**Zn**, Mg, AL, K, Ca, Ti, Fe, Zn, Si, O (99.8)	2.90–3.60	**Cu**, S, O, C (0.22)	3.65–3.90					2.90–3.60	1.15–1.58
6	**Zn**, Fe Ca, K, Mg, Si, O (99.7)	2.90–3.60	**Cu**, S O, C (0.29)	3.65–3.90					2.90–3.60	1.15–1.58
7	**Zn**, Mg, AL, K, Ca, Fe, Si, O (95.7)	2.90–3.60	Mg, AL, S, K, Ca, Ti, Si, O (4.30)	2.90–3.60					2.90–3.60	1.15–1.58
8	**Zn**, Ca, Fe, K, Al, Mg, Si, O (99.9)	2.90–3.60	**Cu**, S, O, C (0.13)	3.65–3.90					2.90–3.60	1.15–1.58
1–2 mm										
9	**Cu**, Fe, O (1 0 0)	5.20–6.50							5.20–6.50	2.55–3.33
10	**Cu,** O (64.5)	6.10–6.50	**Cu, Zn**, O (35.5)	5.50–6.50					5.89–6.50	2.96–3.33
11	**Cu, Zn**, O (68.0)	5.50–6.50	**Zn**, O (32.0)	5.50					5.5–6.18	2.73–3.14
12	**Cu**, S, O (3.81)	3.65	Fe, Ca, Si, O (96.2)	2.90–3.60					2.93–3.60	1.17–1.58
13	**Cu**, Sn, O (5.49)	6.10–6.90	Fe,O (94.5)	5.20–5.30					5.25–5.39	2.58–2.66
14	**Cu**, Sn, O (1.20)	6.10–6.90	Fe, Ca, Si, O (98.8)	2.90–3.60					2.94–3.64	1.18–1.60
15	**Cu**, Fe, S, O (0.40)	3.65	Fe, Si, O (99.6)	2.90–3.60					2.90–3.60	1.16–1.59
16	**Cu**, Sn, O (45.7)	6.10–6.90	Fe, Ca, Si, O (54.3)	2.90–3.60					4.36–5.11	2.04–2.49
17	**Cu**, Fe, S, O (42.0)	3.65	Fe, Si, O (58.0)	2.90–3.60					3.22–3.62	1.34–1.59
18	**Zn**, Fe, Al, O (51.1)	2.90–3.60	Fe, O (48.9)	5.20–5.30					4.02–4.43	1.83–2.08
19	**Cu, Zn**, O (80.0)	5.50–6.50	**Cu**, O (20.0)	6.10–6.50					5.62–6.50	2.8–3.33
20	**Cu**, S, O (0.21)	3.65	**Zn**, Fe, Al, O (1.66)	2.90–3.60	**Zn**, Ca, Si, O (98.1)	2.90–3.60			2.90–3.60	1.15–1.58
21	**Cu**, S, O (0.07)	3.65	**Zn**, Fe, O (0.72)	5.20–5.50	Fe, Ca, Si, O (99.2)	2.90–3.60			2.92–3.61	1.16–1.58
0.250–1 mm										
22	**Cu**, Fe, C, O (1 0 0)	3.90							3.90	1.76
23	**Cu**, O, C (1 0 0)	3.90							3.90	1.76
24	**Cu**, C, O (76.0)	3.90	**Cu**, Si, C, O (24.0)	2.90–3.60					3.66–3.83	1.61–1.71
25	**Cu**, C, O (8.96)	3.90	Ca, C, O (91.0)	2.54					2.66	1.01
26	**Cu**, Fe, C, O (26.7)	3.90	Fe, C, O (73.3)	3.65					3.72–3.73	1.65–1.66
27	**Cu**, C, O (33.4)	3.65	(Al), Si, O (66.6)	2.90–3.60					3.15–3.62	1.3–1.59

Table 4 (*Continued*)

N-P	Elements in P1	d-P1	Elements in P2	d-P2	Elements in P3	d-P3	Elements in P4	d-P4	Mean d	CC
		(g/cm^3)		(g/cm^3)		(g/cm^3)		(g/cm^3)	(g/cm^3)	
28	**Cu**, Fe, C, O (49.3)	3.90	Fe, C, O (50.7)	3.65					3.77	1.68
29	**Cu**, C, O (75.2)	3.90	Fe, C, O (24.8)	3.65					3.84	1.72
30	**Cu**, Fe, C, O (77.9)	3.90	Fe, C, O (12.7)	3.90	Fe, Al, Ca, Na, Si, O (9.37)	2.90–3.60			3.8–3.87	1.7–1.74
31	**Zn**, Fe, Ca, Ti, K, AL, Mg, Si, O (1 0 0)	2.90–3.60							2.90–3.60	1.15–1.58
32	**Zn**, Fe, Ca, Ti, K, Al, Mg, Si, O (96.2)	2.90–3.60	**Cu**, Al, Fe, Ca, Si, C, O, S (3.78)	2.90–3.60					2.90–3.60	1.15–1.58
33	**Zn**, **Cu**, **Fe**, Si, C, O (76.1)	2.90–3.60	**Zn**, Fe, K, Al, O, C (15.5)	2.90–3.60	Fe, C, O (8.38)	3.90			2.98	1.2–1.59
34	**Zn**, **Cu**, Fe, Ca, Ti, K, S, AL, Mg, S, O (92.5)	*	**Zn**, Al, Fe, Ti, Ca, K, Mg, Si, C, O (5.41)	2.90–3.60	**Cu**, Fe, Ca, S, O, C (2.10)	*			*	*
35	**Zn**, **Cu**, **Pb**, Fe, AL, Mn, Si, C, O (2.50)	2.90–3.60	**Cu**, Pb, Fe, Mn, AL, Si, O, C (13.6)	2.90–3.60	K, Fe, Al, Si, O (38.7)	2.90–3.60	Fe, C, O (45.2)	3.90	3.35–3.74	1.43–1.66
36	**Zn**, Fe, Al, Ca, K, Mg, Si, C, O (21.9)	2.90–3.60	Fe, C, O (2.80)	3,96	Fe, Ca, Ti, K, Al, Mg, Si, O (67.5)	2.90–3.60	K, Al, Ti, Si, O (7.86)	2.90–3.60	2.93–3.61	1.17–1.58

Table 5
Densimetric characterization of the 2–4 mm fraction of MSW1, MSW2, MSW3 and MR1.

Soil	Parameter	Mass	Elements (mg/kg)				
		(%)	Ba	Cu	Pb	Sn	Zn
MSW1	Pre-conditionned	100	360±18	599±96	487±66	176±11	486±32.7
	Treated	93.3	327±13	128±24	239±55	38.4±10.0	374±57.7
	Mass removal[a] %	**6.67**	**15.2**	**80.0**	**54.1**	**79.7**	**28.2**
MSW2	Pre-conditionned	100	601±105	759±196	1170±240	384±98	926±106
	Treated	85.5	450±17	262±26	629±113	216±17	767±178
	Mass removal %	**14.5**	**35.8**	**70.4**	**54.0**	**51.9**	**29.1**
MSW 3	Pre-conditionned	100	619±125	810±267	1950±656	539±126	797±131
	Treated	71.9	729±34	232±33	662±51	126±15	864±60
	Mass removal %	**28.1**	**15.3**	**79.4**	**75.5**	**83.2**	**22.0**
MR1	Pre-conditionned	100		3540±370			5480±660
	Treated	47.8		678±97			335±79
	Mass removal %	**52.2**		**90.9**			**97.1**

[a] Mass removal = The mass removed of the concentrate and metals removal calculated according to the mass balance (Eqs. (3) and (5)).

thereby generated. The soil fractions of 2–4 mm, 1–2 mm, and 0.25–1 mm were treated by attrition scrubbing. This was performed at 1500 r/min at room temperature for 10 min with a solid-liquid ratio fixed at 30% (by weight). For the 2–4 mm, 1–2 mm, and 0.25–1 mm of MSW3 and MR1, a supplement pre-treatment was used during the attrition scrubbing process in order to prevent the eventual effect of organic contaminants on subsequent physical treatments based on previous works (Bisone et al., 2013, Jobin et al., 2016a). Attrition sludge was removed from the contaminated soils using 2 mm, 1 mm, and 0.25 mm sieves for the soil fractions of 2–4 mm, 1–2 mm, and 0.25–1 mm, respectively. The soil fractions <0.25 mm and the generated sludge were recommended for disposal via a landfill. Pre-conditioned fractions were collected and exhaustively characterized before being processed using a wet shaking table (for fractions of 1–2 mm and 0.25–1 mm) or jig (for fractions of 2–4 mm).

2.2.2. Feedstock characterization

Previous research has reported the usefulness of densimetric and mineralogical characterization of soils contaminated with MSW incinerator ashes in predicting the efficiency and limitations of gravimetric processes including wet shaking and jig treatment (Mercier et al., 2001, Mouedhen et al., 2018). In addition, according to Mouedhen et al. (2018), DMS was useful in optimizing the use of a wet shaking table to treat soil fractions of 1–2 mm and 0.25–1 mm contaminated with MSW ashes. In the same context, to study the effectiveness of densimetric characterization for optimizing the use of the jig, DMS using tetrabromoethane (density = 2.9 g/cm^3) was used to characterize the density distribution of the soil fraction of 2–4 mm. DMS was performed using 200 g of each soil sample, obtained using riffle-type sample splitters. The mass of the different products (<2.9 g/cm^3 and >2.9 g/cm^3) and the corresponding chemical compositions and densities were then determined.

Table 6
Physical and chemical results of jigging treatment of 2–4 mm fractions derived from MSW1, MSW2, MSW3 and MR1.

Soil	Parameter	Mass	Ba	Cu	Pb	Sn	Zn
		(%)	(mg/kg)	(mg/kg)	(mg/kg)	(mg/kg)	(mg/kg)
MSW1	Pre-conditionned	100	360	599	487	176	486
	Treated	89.4	392	196	385	107	620
	Mass removal[a] %	**10.6**	**2.60**	**70.8**	**29.3**	**45.9**	**0.00**
	R_E[b]	1.59					
	R_M[c]		0.251	0.885	0.542	0.576	–
MSW2	Pre-conditionned	100	601	759	1170	383	926
	Treated	87.1	549	406	815	327	993
	Mass removal %	**12.9**	**20.5**	**53.4**	**39.4**	**25.6**	**6.55**
	R_E	0.89					
	R_M		0.572	0.758	0.730	0.494	0.225
MSW3	Pre-conditionned	100	619	810	1950	539	797
	Treated	70.0	695	575	897	432	1120
	Mass removal %	**30.0**	**21.4**	**50.3**	**67.7**	**44.0**	**1.83**
	R_E	1.07					
	R_M		1.40	0.634	0.897	0.529	0.08
MR1	Pre-conditionned	100	3540				5480
	Treated	56.9	2160				2880
	Mass removal %	**43.1**	**65.3**				**70.1**
	R_E	0.826					
	R_M		0.719				0.722

[a] Mass removal = The mass removed of the concentrate and metals removal calculated according to the mass balance (Eqs. (3) and (5)).

[b] R_E = Removal efficiency (Eq. (2)).

[c] R_M = Metal removal efficiency (Eq. (4)).

In order to examine the mineralogy of contaminants in soil fractions of 2–4 mm, 1–2 mm, and 0.25–1 mm and to study the applicability of gravimetric separation techniques, thin sections (0.05 μm) of concentrates (>2.9 g/cm³) obtained from TBE separation were prepared. The thin sections were coated with gold using a sputter coater system (SPI™ Module TM Sputter-Coater, 11430-AB). Scanning electron microscopy coupled with a qualitative chemical analysis was performed using a Carl Zeiss microscope (EVO®50) equipped with an X-ray energy dispersion spectrometer (Oxford Instruments, INCA EDS; INCAx-sight detector). The accelerating voltage and the beam current were fixed at 20 kV and 100 μA, respectively. Particles were scanned in the backscattered electron mode to locate both the contaminated and heavy metal-bearing phase, the surfaces of which were measured using Mesurim_Pro software. The mineralogy as well as the density of each phase was estimated based on elements identified by the X-ray analysis. For each particle, the mean density was calculated by considering the surface ratio of the contaminated phase and the heavy metal-bearing phase.

The elemental composition of metals present in soil fractions of 2–4 mm, 1–2 mm, and 0.25–1 mm for the studied soils was investigated. For each sample, the chemical composition including the levels of Ba, Cu, Sn, and Zn was determined before and after treatment. For this, soil samples were finely grinded (∼80 μm) and mineralized according to the "aqua regia" protocol defined by the Centre d'Expertise en Analyse Environnementale du Québec (CEAEQ; MA. 100 – Lix. com.1.1) (CEAEQ, 2010). SC0063618, LKSD-2, and LKSD-4 were used to validate the digestion method. The resulting liquids were analyzed by inductively coupled plasma atomic emission spectroscopy (Varian, Vista AX CCD simultaneous ICP-AES system). The density parameter was continually determined during the experiments using a helium pycnometer (Micrometrics, AccuPyc II 1330).

2.3. Mineral processing

2.3.1. Soil fraction >4 mm

For each sample, the fraction of soil >4 mm was treated using magnetic separation to adequately separate the ferri/ferro magnetic fraction from the non-magnetic fraction. To do so, based on particles sizes, 4 kg of the soil fraction >12 mm and 3 kg of the 4–12 mm fraction were randomly sub-sampled to ensure maximum representativeness of the samples. Each sub-sample was then spread on a flat surface, and ferrous particles were separated from non-ferrous particles using a hand magnet (0.3 T) positioned at a height of a few millimeters. The mass of metals was then determined. The separated non-ferrous particles were then crushed with a jaw crusher (Fritsch, Pulverisette 1) and subjected to chemical analysis.

2.3.2. 2–4 mm soil fraction

A Denver laboratory mineral jig (tank volume = 140 cm³) was used for concentrating heavy metals contained within the soil fractions of 2–4 mm. The bed was composed of 15 g of silicon nitride balls (height = 5.6 mm, density = 3.2 g/cm³). The feed water flow and the feed solid flow were fixed at 3.5 L/min and 100 g/min, respectively. Approximately 800 g of dry soil samples were fed using a vibratory feeder (Fritsch, Laborette 24). For each soil sample, the number of runs was defined based on the mass and density of the concentrates measured. After each run, the R_E ratio was determined according to Eqs. (2) and (3) in order to compare the performance of the jig with that of DMS (optimal treatment). If the mass of the cumulative concentrate was lower than that obtained by DMS ($R_E < 1$), a supplementary run was performed under the same conditions. Thus, the end of the jig treatment was marked by a mass of high-density concentrate close to that obtained by DMS ($R_E \sim 1$).
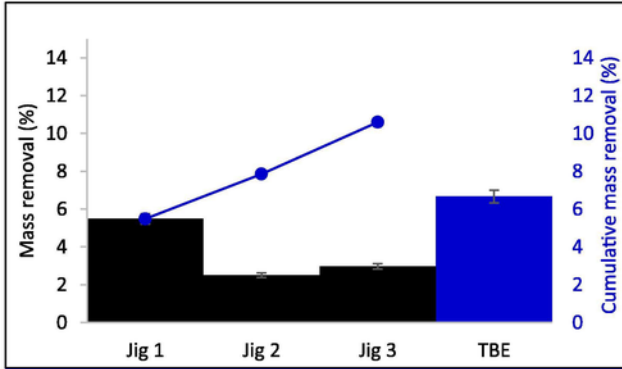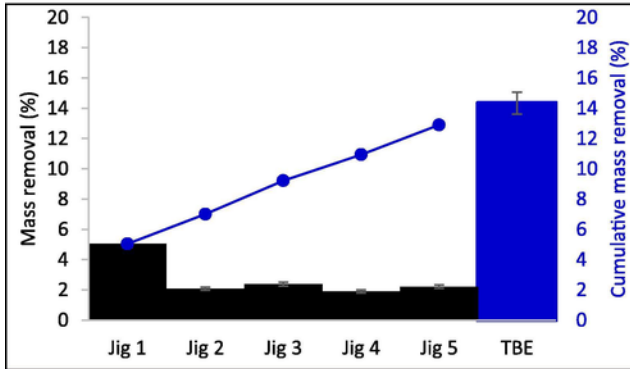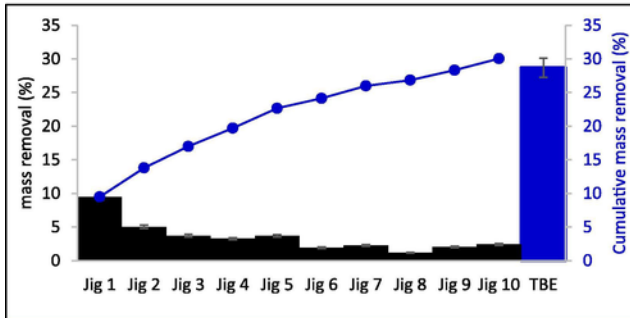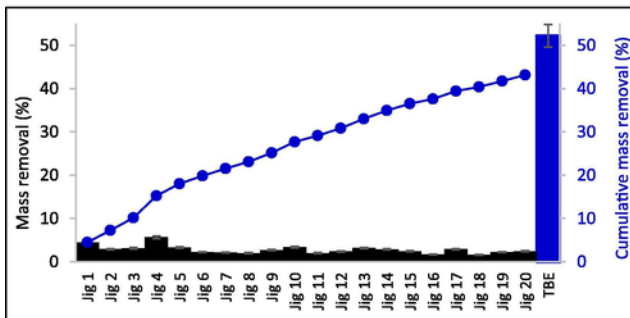
MSW1, R_E=1.57

MSW2, R_E=0.90

MSW3, R_E= 1.07

MR1, R_E= 0.83

Fig. 2. The mass of concentrate removed from the 2–4 mm fractions of MSW1, MSW2, MSW3 and MR1 during each jigging batch and after "n" jigging batches.

Mass removal efficiency ratio

$$R_E \ ratio = \frac{Total \ mass \ proportion \ of \ concentrate \ remov}{Total \ proportion \ of \ concentrate \ removed \ by \ dense}$$

Total mass proportion of concentrate removed via dense media separation or jig (%)

$$C_{removal} \ (\%) = 100 * \left(1 - \frac{Mass \ of \ light \ particles \ (g)}{Total \ mass \ (g)}\right) \quad (3)$$

At the end of the jig treatment, the metal removal efficiency ratio (R_M) was calculated (Eqs. (4) and (5)). R_M enabled the comparison of metal removal by the jig and by DMS to assess the maximum efficiency of the gravimetric device in removing a metal 'M' when $R_E \sim 1$.

Metal removal efficiency ratio

$$R_M = \frac{"M" \ removal \ by \ jig \ (\%)}{"M" \ removal \ by \ dense \ media \ separation \ (\%)} \quad (4)$$

The mass of metal "m" removed via dense media separation or jig (%)

$$M_{removal} \ (\%) = 100 * \left(1 \ \frac{Mass \ of \ metal \ "M" \ obtained \ at \ light \ fraction \ of \ the \ samp}{Total \ mass \ (g)}\right.$$

2.3.3. Soil fraction of 0.25–2 mm

A Wilfley laboratory table (Outokumpu Technology, 13A-SA), characterized by 1.02 m of length and 0.46 m of width was used to separately treat the soil fractions of 0.25–1 mm and 1–2 mm. Previous work by Mouedhen et al. (2018) highlighted that a complete characterization of soil samples and the realization of only five trials on the device were necessary to maximize the recovery of metals from the 0.25–1 mm fraction of MSW2, through one passage on the device. According to preliminary testing, five trials were performed on each sample to define the optimal treatment settings for the wet shaking table (i.e., tilt, stroke length and frequency, and wash water flow). The dry feedstock was introduced using a vibratory feeder. For all experiments, the solid flow rate was set at 100 g/min and the feed water flow rate was fixed at 2 L/min. Optimal settings of tilt (°), stroke length (mm), stroke frequency (strokes/min), and wash water flow (L/min) were as follow:

- 1–2 mm soil fraction of MSW1: 12°, 12 mm, 375 S/min, and 5.5 L/min;
- 0.25–1 mm sol fraction of MSW1: 11°, 11 mm, 352 S/min, and 5 L/min;
- 1–2 mm soil fraction of MSW2: 10.5°, 11 mm, 432 S/min, and 6 L/min;

Table 7
. Physical process efficiency in treating MSW1.

Sample	Treatment	Parameters	Mass	Inorganic elements (mg/kg)				
			(%)	Ba	Cu	Pb	Sn	Zn
Bulk soil		**100**	**550**	**341**	**852**	**199**	**932**	
>12 mm	Water washing and Magnetism	Initial	22.4	406	108	273	46.9	969
		Treated	18.6	222	42.3	119	11.9	118
		Mass removal[a] %	**17.0**	**54.6**	**67.4**	**64.0**	**79.0**	**89.9**
4–12 mm	Water washing and Magnetism	Initial	19.4	375	513	569	177	677
		Treated	15.1	273	479	491	46	424
		Mass removal %	**22.5**	**43.5**	**27.6**	**33.0**	**79.8**	**51.5**
2–4 mm	Attrition scrubbing and Jig	Initial	11.0	489	589	783	284	935
		Treated	5.62	360	599	487	176	486
		Mass removal %	**48.9**	**62.4**	**48.0**	**68.2**	**68.3**	**73.4**
1–2 mm	Attrition scrubbing and Wet shaking table	Initial	7.00	529	458	1210	332	953
		Treated	4.68	451	240	559	129	687
		Mass removal %	**33.1**	**43.1**	**65.0**	**69.1**	**74.0**	**51.9**
0.250–1 mm	Attrition scrubbing and Wet shaking table	Initial	17.0	324	183	942	175	514
		Treated	12.4	229	168	466	111	480
		Mass removal %	**26.8**	**48.3**	**32.8**	**63.8**	**53.6**	**31.7**
<0.250 mm	Safe disposal	Initial	23.2	1030	385	1600	299	1410
		Treated	–	–	–	–	–	–
		Mass removal %	**100**	**100**	**100**	**100**	**100**	**100**
Treated soil			**56.4**	**270**	**259**	**368**	**69**	**364**
Mass removal from the >0.250 mm soil fraction (%)			**26.6**	**50.8**	**42.1**	**58.7**	**69.9**	**66.1**
Mass removal from total soil (%)			**43.6**	**72.3**	**57.3**	**76.2**	**80.4**	**78.0**

[a] Mass removal = The mass removed of the concentrate and metals removal calculated according to the mass balance (Equations (3) and (5)).

Table 8
Physical process efficiency in treating MSW2.

Sample	Treatment	Parameters	Mass	Inorganic elements (mg/kg)				
			(%)	Ba	Cu	Pb	Sn	Zn
Bulk soil			100	572	569	1080	416	1200
>12 mm	Water washing and Magnetism	Initial	31.0	262	474	396	225	593
		Treated	20.5	106	67.7	86.3	11.1	125
		Mass removal[a] %	**33.7**	**73.0**	**90.5**	**85.6**	**96.7**	**86.0**
4–12 mm	Water washing and Magnetism	Initial	15.1	430	279	616	191	917
		Treated	10.5	267	383	450	38	332
		Mass removal %	**30.2**	**56.6**	**4.1**	**48.9**	**86.2**	**74.7**
2–4 mm	Attrition scrubbing and Jig	Initial	10.9	726	918	1740	474	1360
		Treated	5.98	549	406	815	327	993
		Mass removal %		**58.5**	**75.7**	**74.3**	**62.1**	**59.8**
1–2 mm	Attrition scrubbing and Wet shaking table	Initial	7.10	643	727	1640	596	1290
		Treated	4.62	536	378	795	315	996
		Mass removal %	**34.9**	**45.7**	**66.2**	**68.4**	**65.5**	**49.7**
0.250–1 mm	Attrition scrubbing and Wet shaking table	Initial	16.0	445	463	1660	628	1200
		Treated	12.1	385	304	719	475	783
		Mass removal %	**24.7**	**34.9**	**50.6**	**67.4**	**43.1**	**50.8**
<0.250 mm	Safe disposal	Initial	19.8	1164	778	1480	620	2240
		Treated	–	–	–	–	–	–
		Mass removal %	**100**	**100**	**100**	**100**	**100**	**100**
Treated soil			53.7	287	247	442	182	485
Mass removal from the >0.250 mm %			**32.9**	**55.0**	**68.0**	**69.9**	**66.7**	**65.4**
Mass removal from the total soil (%)			**46.3**	**73.1**	**76.7**	**78.1**	**76.5**	**78.2**

[a] Mass removal = The mass removed of the concentrate and metals removal calculated according to the mass balance (Eqs. (3) and (5)).

- 0.25–1 mm soil fraction of MSW2: 11°, 11 mm, 352 S/min, and 5 L/min;
- 1–2 mm soil fraction of MSW3: 11°, 12.5 mm, 300 S/min, and 4 L/min;
- 0.25–1 mm soil fraction of MSW3: 10.5°, 11 mm, 432 S/min, and 6 L/min;
- 1–2 mm soil fraction of MR1: 12°, 12 mm, 375 S/min, and 5·5 L/min;
- 0.25–1 mm soil fraction of MR1: 11°, 11 mm, 353 S/min, and 5 L/min.

The mass of generated products, the corresponding densities, as well as the residual concentration of metals present in treated samples, were evaluated in order to determine the performance of the wet shaking table.

Table 9
Physical process efficiency in treating MSW3.

Sample	Treatment	Parameters	Mass	Inorganic elements (mg/kg)				
			(%)	Ba	Cu	Pb	Sn	Zn
Bulk soil			100	1000	1160	2010	784	1630
>12 mm	Water washing and Magnetism	Initial	14.7	483	1290	688	289	470
		Treated	11.4	205	27	133	15	175
		Mass removal[a] %	**22.1**	**66.9**	**98.4**	**84.9**	**95.9**	**82.8**
4–12 mm	Water washing and Magnetism	Initial	21.0	699	1620	1700	977	1340
		Treated	12.5	484	1390	503	99	664
		Mass removal %	**40.3**	**58.6**	**48.6**	**82.3**	**93.9**	**70.5**
2–4 mm	Attrition scrubbing and Jig	Initial	19	700	1120	1820	703	1440
		Treated	8	695	575	897	432	1120
		Mass removal %	**58.8**	**59.1**	**78.9**	**79.7**	**74.8**	**68.1**
1–2 mm	Attrition scrubbing and Wet shaking table	Initial	8	1087	1120	3030	1170	1810
		Treated	4	480	364	961	340	849
		Mass removal %	**54.8**	**80.0**	**85.4**	**85.7**	**86.9**	**78.8**
0.250–1 mm	Attrition scrubbing and Wet shaking table	Initial	20	1050	702	2000	716	1510
		Treated	12	620	318	889	362	934
		Mass removal %	**41.1**	**65.2**	**73.3**	**73.8**	**70.2**	**63.6**
<0.250 mm	Safe disposal	Initial	17	2059	1070	3240	950	3230
		Treated	–	–	–	–	–	–
		Mass removal %	**17**	**100**	**100**	**100**	**100**	**100**
Treated soil			47	485	579	611	218	702
Mass removal from the >0.250 mm (%)			**42.9**	**64.7**	**71.9**	**80.1**	**83.4**	**69.2**
Mass removal from the total soil (%)			**52.7**	**77.2**	**76.4**	**85.6**	**86.9**	**79.6**

[a] Mass removal = The mass removed of the concentrate and metals removal calculated according to the mass balance (Eqs. (3) and (5)).

3. Results and discussion

3.1. Chemical characterization

Table 2 shows the concentrations of metals and their proportions in different soil fractions of MSW1, MSW2, MSW3, and MR1.

Total metal analysis in bulk soils showed that MSW3 was the most contaminated (Ba = 1000 mg/kg, Cu = 1160 mg/kg, Pb = 2010 mg/kg, Sn = 784 mg/kg, and Zn = 1630 mg/kg) followed by MSW2 and MSW1. MR1 was highly contaminated with Cu (3060 mg/kg) and Zn (3110 mg/kg). According to the mass balance, heavy metals were heterogeneously distributed in the different soil fractions. However, for MSW1, MSW2, MSW3, and MR1, the majority of contaminants were concentrated in the soil fraction <0.25 mm. Consequently, volume reduction of the soil fraction <0.25 mm can potentially contribute to reducing a portion of inorganic contamination in these soils.

In order to define the most problematic fractions, a comparison was made with the heavy metal limits imposed by the Land Protection and Rehabilitation Regulation in the province of Quebec, Canada (MDDELCC, 2017); based on category C criteria, soil cannot be used when the concentrations of metals are higher than the following: Cu = 500 mg/kg, Pb = 1000 mg/kg, Sn = 300 mg/kg, and Zn = 1500 mg/kg. These are the limits placed on commercial or industrial use. If these limits are exceeded, appropriate management is required. Since safe disposal is required for the soil fraction <0.25 mm, this fraction was not considered. Consequently, in the case of MSW1, Cu, Pb, and Sn were slightly above category C limits in both the soil fractions of 2–12 mm and 1–2 mm. For MSW2, the soil fraction of 0.25–4 mm was the most problematic fraction, containing large concentrations of Pb and Sn. A high concentration of Cu was also observed in the soil fraction of 1–4 mm. In the case of MSW3, the soil fraction >0.25 mm was entirely problematic because of the high concentration of Cu. The concentrations of Pb and Sn were also very high in the 0.25–12 mm soil fraction, while the con-

centration of Zn was high in the 0.25–2 mm fraction. Cu and Zn were excessively high in MR1 in all fractions. Consequently, appropriate treatments are required for soils from these sites if potential reuse for commercial/industrial (<criteria C) or residential purposes (<criteria B) is to be considered.

3.2. Mineralogical characterization

Tables 3 and 4 show the mineralogical analysis of the 2–4 mm, 1–2 mm, and 0.25–1 mm fractions of soils contaminated by MSW ashes and by metallurgical residues. These data highlight the elemental composition of each examined heavy particle. The surface of contamination and metal-bearing phases, estimated mean density of the particles, and concentration criterion are also shown.

Firstly, particles derived from MSW ashes showed both homogenous and heterogeneous mineralogical properties owing to the presence of mono/multi mineralogical phases. Such a typical complexity in the composition of contaminated particles is the result of initial heterogeneous composition of waste, thermal transformations of metals in a multi-component system during the incineration process (i.e., complete/partial melting, oxidation, and surface intergrowth of melted pieces with mineral components), and geochemical transformations in soil (Kabata-Pendias, 2011, Kowalski et al., 2017, Shen et al., 2003). By studying surface proportions of metal-carrying phases and metal-bearing phases, several scenarios were distinguished.

In the 0.25–1 mm, 1–2 mm, and 2–4 mm soil fractions, Pb, Sn, and Cu were mainly found in totally liberated phases. Most Pb, Sn, and Cu oxides present were identified and their mineralogical forms were as follows: $Pb_aAl_bC_dO_e$, Pb_aO_b, $Pb_aSn_bO_c$, Pb_aFeO_b, Pb_aO_b-$Pb_aSn_bO_c$, Pb_aO_b-$Pb_aFe_bPO_c$-$Pb_aZn_bO_c$, Pb_aO_b-$Pb_aAl_bSb_cO_d$, SnO, Sn_aFe_b-$Sn_aFe_bC_cO_d$, Sn_aFe_b-$Sn_aFe_bC_cO_d$, Cu_aO_b, Cu_aO_b-$Cu_aFe_bO_c$, $Cu_aSn_bO_c$, and $Cu_aAl_bO_c$-$Cu_a(Cl/O)_b$. Contaminants found associated with the reducible fraction (Fe oxides) are quite mobile and reflect anthropogenic sources (Sungur et al., 2019). In fact, Cu, Pb, Sn, and Zn oxides are used in the manufacture of bat-

Table 10
Physical process efficiency in treating MR1.

Sample	Treatment	Parameter	Mass (%)	Inorganic elements (mg/kg) Cu	Inorganic elements (mg/kg) Zn
Bulk soil			100	3060	3110
>12	Water washing and Magnetism	Initial	20.6	1570	963
		Treated	16.9	872	1040
		Mass removal[a] %	**17.7**	**54.2**	**10.9**
4–2 mm	Water washing and Magnetism	Initial	13.8	2550	3410
		Treated	11.3	1780	3770
		Mass removal %	**18.4**	**43.0**	**9.57**
2–4 mm	Attrition scrubbing and Jig	Initial	22.6	2940	4850
		Treated	9.45	2160	2880
		Mass removal %	**58.3**	**69.3**	**75.2**
1–2 mm	Attrition scrubbing and Wet shaking table	Initial	10.5	4190	5390
		Treated	5.55	1590	1970
		Mass removal %	**47.2**	**80.0**	**80.8**
0.250–1 mm	Attrition scrubbing and Wet shaking table	Initial	14.5	3300	2100
		Treated	10.0	1400	1370
		Mass removal %	**31.2**	**70.9**	**55.0**
<0.250 mm	Safe disposal	Initial	18.0	4430	2640
		Treated	0.00	0.00	0.00
		Mass removal %	**100**	**100**	**100**
Treated soil			53.2	1470	2110
Mass removal from the >0.250 mm (%)			**35.2**	**65.5**	**57.6**
Mass removal from the total soil (%)			**46.8**	**74.5**	**64.0**

[a] Mass removal = The mass removed of the concentrate and metals removal calculated according to the mass balance (Eqs. (3) and (5)).

teries, printed circuit boards, drink and food containers, paints, plastics, glasses, and pesticides (Chandler et al., 1997; Wei et al., 2011). The estimated mean densities of these particles ($3.90–9.90\,g/cm^3$) as well as the concentration criterion (1.76–4.88) were high, indicating a potentially positive response to gravimetric separation processes. Furthermore, Sn and Cu phases were found bound by iron oxide phases, e.g., $Sn_aFe_b\text{-}Fe_aO_b$, $Sn_aO_b\text{-}Fe_aO_b$, $Sn_aFe_bC_cO_d\text{-}Fe_aO_b$, $Cu_aSn_bFe_c\text{-}Sn_aFe_bO_c$, $Sn_aFe_bO_c\text{-}Fe_aO_b$, $Sn_aFe_bBr_cO_d\text{-}Fe_aO_b$, $Sn_aFe_bO_c\text{-}Fe_aAl_bO_c\text{-}Al_aO_b$, and $Cu_aC_bO_c\text{-}Fe_aC_bO_c$. Steel and iron generally oxidize in the combustion furnace. Magnetite (Fe_3O_4), hematite (Fe_2O_3), and wüstite (FeO) were previously identified as the mineralogical forms of Fe_aO_b in bottom ashes (Chimenos et al., 1999). The density of these minerals is around $5\,g/cm^3$ (Min.Database, 2018). Consequently, independent of the surface occupied by such pollutant-bearing phases, contaminated particles are generally characterized by a high mean density ($3.90–9.00\,g/cm^3$). Likewise, the relative concentration criterion was generally higher than 1.76, which promotes separation when using gravimetric devices. In other groups of particles, Pb was entrapped within a silica matrix. This form of contaminants is immobile and can be the result of both the weathering of rock minerals and the transformation of Pb during the incineration process (Dong et al., 2015; Sungur et al., 2019). This was found bound in $\text{-}Pb_aFe_bCa_cO_d$ phases or in $\text{-}Fe_aO_b$ phases. In other cases, the silica matrix was bound to Pb-carbonate ($\text{-}Pb_aSn_bC_cO_d$ and $\text{-}Pb_aC_bO_c\text{-}Fe_aC_bO_c$), Pb-oxide/chloride ($\text{-}Pb_aO_bPb_bCl_c\text{-}Fe_aO_b$ and $\text{-}Pb_aFe_bO_c\text{-}Al_aO_b$), or Cu-carbonate ($\text{-}Cu_aFe_bC_cO_d\text{-}Fe_aO_b$) phases. Prior work has identified the silica matrix as silica amorphous glass. Derivative mineralogical phases of feldspars have also been identified, such as anorthite ($CaAl_2Si_2O_8$, $2.73\,g/cm^3$). Furthermore, the presence of quartz (SiO_2, $2.62\,g/cm^3$), melilite groups such as gehlenite ($Ca_2Al_2SiO_7$, $2.98\,g/cm^3$), and calcium silicate minerals such as larnite (Ca_2SiO_4, $3.28\,g/cm^3$) have also been identified (Chandler et al., 1997, Wei et al., 2011). Consequently, the fate of such groups of contaminated particles undergoing a gravimetric separation depends on two major aspects, specifically, the nature of the silica matrix and the surface proportion of each phase composing the contaminated particle. For instance, in the case of particle 48, $Pb_aC_bO_c$ (cerussite) is found bound in a silica phase that occupies up to 65% of the total surface of the particle. Knowing that the density of this comprises between 2.90 and $3.60\,g/cm^3$, the mean density of this particle can be lowered to $3.57\,g/cm^3$. This leads to a concentration criterion equivalent of 1.57, hence making the gravimetric separation difficult. Moreover, calcium carbonate was determined as a bearing phase of Sn-oxide ($Sn_aO_b\text{-}Ca_aO_b$). Calcite, characterized as having a low density ($2.54\,g/cm^3$), was deemed to originate from marble used as a building material (Chimenos et al., 1999). If this significantly contributes to the total surface of contaminated particles, mean densities decrease and the efficiency of separation when using gravimetric devices is reduced.

The microscopic examination of the 0.25–1 mm, 1–2 mm, and 2–4 mm soil fractions of MR1 showed several mineralogical scenarios of Cu and Zn particles. The first group identified contained totally liberated Cu and Zn carbonates/oxides, namely $Cu_aFe_bC_cO_d$, $Cu_aZn_bO_c\text{-}Zn_aO_b$, $Cu_aO_b\text{-}Cu_aZn_bO_c$, and $Cu_aFe_bO_c$. Some contaminated particles showed Cu and Zn found bound in heavy phases of Fe-carbonate/oxide, i.e., $Cu_aFe_bC_cO_d\text{-}Fe_aCbO_c$, $Cu_aSn_bO_c\text{-}Fe_aO_b$, and $Zn_aO_b\text{-}Fe_aO_b$. As mentioned above, gravimetric separation is generally favored by such groups (concentration criterion >1.76; $3.90–6.50\,g/cm^3$). The second group of particles showed Cu and Zn as entrapped inclusions within a silica matrix bound in a Fe-carbonate phase or in Zn, Fe, K, Al-carbonates phases. Depending on the corresponding surface of the latter, the mean density of contaminated particle could be increased, which then favored gravimetric separation (e.g., particle 35). In addition, Cu-carbonate/oxide/sulfates were found bound in silica matrix phases, i.e., $Cu_aC_bO_c\text{-}Si\text{-phase}$, $Cu_aC_bO_c\text{-}Si\text{-phase}$ containing Cu and Zn inclusions, $Cu_aSbO_c\text{-}Si\text{-phase}$, $Cu_aSn_bO_c\text{-}Si\text{-phase}$, and $Cu_aFe_bO_c\text{-}Si\text{-phase}$. This group depicted the typical composition of slags. In fact, ferrous slags are known to be mainly composed of silicates, aluminosilicates, and calcium alumina silicates (Ramachandra Rao, 2006). Further research has specified olivine group silicates ($3.34\,g/cm^3$), melilite group silicates ($2.95\,g/cm^3$), Ca-silicates ($3.28\,g/cm^3$), quartz ($2.62\,g/cm^3$), cristobalit ($2.30\,g/cm^3$), and glass as frequently present in steel and ferrous slags (Piatak et al., 2015b). Accordingly, the fate of this third group of contaminated particles closely depends on the Cu-carrying surface and on the nature of the silica matrix. Other Cu particles showed Cu carbonates found bound to a calcite phase ($Cu_aC_bO_c\text{-}Ca_aC_bO_c$), strongly reducing the mean density of the particle as well as the concentration criterion. The presence of this kind of group can lower the efficiency of gravimetric separation techniques. Cu and Zn were frequently co-present in contaminated particles. Similar behavior of Cu and Zn particles during the gravimetric treatment of MR1 was therefore expected.

3.3. Performance of the DMS (optimal scenario) at removing inorganic contaminants

Previous research has discussed the usefulness of densimetric characterization (DMS) in predicting the performance of wet shaking tables and for optimizing the parameters of gravimetric devices to separate metals from the 1–2 mm and 0.25–1 mm fractions of MSW1, MSW2, MSW3, and MR1. Metals such as Cu, Pb, and Sn were successfully removed from the 0.25–2 mm fraction of soils contaminated by MSW ashes when subjected to a TBE separation process (with 47.5%–94.7% of metals being removed). DMS was also efficient at removing Cu and Zn from the 1–2 mm and 0.25–1 mm fractions of MR1, with removal yields higher than 87.9%.

The proportion of heavy metals in the 2–4 mm fraction of soils was also determined. The corresponding results are presented in Table 5. According to the results obtained, 6.67%, 14.5%, and 28.1% (by weight) of the metallic concentrates were removed from the 2–4 mm fraction of MSW1, MSW2, and MSW3, respectively. The examination of treated fractions showed that the concentrations of Cu, Pb, and Sn significantly decreased. The final concentration of Cu varied from 128 ± 24 to 262 ± 26 mg/kg. The final concentration of Pb varied from 239 ± 55 to 662 ± 51 mg/kg and that of Sn varied from 38.4 ± 10.6 to 216 ± 17 mg/kg. Metal removal yields were moderate to high, ranging from 51.9% to 83.2%, depending on the contaminant. However, removal yields obtained for Zn were very low (22.0%–29.1%). The residual Zn concentration in the 2–4 mm treated fraction varied from 374 ± 58 to 864 ± 23 mg/kg. Likewise, Ba removal was low to moderate for the 2–4 mm fraction (15.2%–35.8%). Concentrations of Ba remained relatively high, ranging from 327 ± 12 to 729 ± 34 mg/kg. Regarding Zn, as shown in Table 4, the microscopic examination showed that Zn/Zn oxide was embedded in a silica matrix. Zn oxide was also found bound in a calcite phase. The presence of such light phases can reduce the mean density of Zn particles and thereby limit the performance of the gravimetric separation process. The heavy fraction constituted half of the 2–4 mm fraction of MR1 (52.2%, by weight). The TBE separation allowed the removal of more than 90% of Cu and Zn, the final concentrations of which decreased to 678 ± 97 mg Cu/kg and 335 ± 79 mg Zn/kg.

Based on both the mineralogical and physical characterization results, satisfactory Cu, Pb, and Sn removal yields are expected if using gravimetric devices to treat the 0.25–1 mm, 1–2 mm, and 2–4 mm fractions of soils contaminated by MSW ashes. Low to moderate efficiencies of separating Ba and Zn are expected. Regarding MR1, satisfactory Cu and Zn removal yields are also expected when using gravimetric separation to treat the 0.25–1 mm, 1–2 mm and 2–4 mm soil fractions.

3.4. Mineral processing technology efficiency

3.4.1. Jig optimization for treating pre-conditioned 2–4 mm fraction of soils

Prior to jig optimization, attrition scrubbing, known to promote the efficiency of gravimetric processes (Dermont et al., 2008) was performed on the 2–4 mm soil fraction (results not shown). The attrition scrubbing removed 37.0%, 42.9% and 42.8% (by weight) of contaminated sludge from the 2–4 mm fractions of MSW1, MSW2, and MSW3, respectively. The high volumes of contaminated sludge can be explained by a positive existing correlation with particle size. In fact, the disintegration of agglomerated particles is generally important during the attrition of coarse soil fractions (Jobin et al., 2015). The levels of heavy metals after attrition scrubbing ("pre-conditioned") can be seen in Table 6. The concentrations of Ba, Pb, Sn, and Zn in MSW1; Ba, Cu, Pb, Sn, and Zn in MSW2; and Ba, Cu, Sn, and Zn in MSW3 were significantly reduced (with an error threshold of 5%). In the case of the 2–4 mm fraction of MR1, a lower mass of sludge was generated next to the pre-treatment (26.7%, by weight). The concentration of Cu was slightly reduced. However, no effect was observed in decreasing the concentration of Zn. Indeed, as can be seen in Supplementary Fig. 1, some Cu phases were found embedded in the total volume of the 2–4 mm particle fraction. Moreover, the microscopic analysis revealed the inclusion of Zn in the silica matrix. Both Cu and Zn were consequently only slightly exposed to the abrasive forces of the attrition scrubbing reactor.

Fig. 2 depicts the mass of concentrate removed from the 2–4 mm fractions of MSW1, MSW2, MSW3, and MR1 during each jigging batch as well as the cumulative mass removed from the concentrate after n jigging batches, where n corresponds to the number of times the sample is required to pass through the jig to remove a mass of concentrate close to that obtained via DMS ($R_E \sim 1$).

Each time the sample was passed through the gravimetric device a small quantity of metals was removed corresponding to a mean value of $2.72 \pm 1.30\%$ (by weight)/pass/soil. For each soil, the density of concentrate was generally maintained high until the sample was passed n number of times, indicating, consequently, a high purity of the heavy separated product (mean density >2.90 g/cm^3). Considering $R_E \sim 1$ as the end of the jigging treatment, positive linear tendency between the initial mass content of heavy metals and the number of passes required can be concluded; 3, 5, 10, and 20 passes through the gravimetric device were required to treat the 2–4 mm fractions of MSW1, MSW2, MSW3, and MR1, respectively. Results of the chemical analysis performed on the treated fraction from the last pass through the jig are presented in Table 6.

Satisfactory removal yields of Cu from the 2–4 mm fractions of MSW1, MSW2, MSW3, and MR1 were obtained, ranging from 50.3% to 70.8%. The R_M (Cu) ratios were higher than 0.634, reflecting removal yields close to those obtained when using TBE separation. The Pb removal yields from the 2–4 mm fractions of MSW1, MSW2, and MSW3 corresponded to 29.3%, 39.4%, and 67.7%, respectively, whereas Sn removals were 45.9%, 25.6%, and 44.0%, respectively. As for Cu, the jig efficiently removed Pb and Sn compared with the TBE separation test (R_M [Pb, Sn] varied from 0.494 to 0.897). Zn was efficiently separated from the 2–4 mm fraction of MR1 using the jig. TBE separation demonstrated similar removal yields (R_M [Zn] = 0.722). According to our observations, Zn followed the behavior of Cu under the jig treatment, confirming the predicted behavior of both densimetric and microscopic characterizations.

The current results are consistent with those described in previous research. Indeed, the jig effectively extracted Pb, Cu, and Sn from the 2–4 mm (>40% removal) and the 0.85–2 mm (43% and 89% removal) soil fractions with different levels of contamination from MSW ashes (Jobin et al., 2015; Mercier et al., 2002). The gravimetric device showed limited capacity for removing Zn and Ba from 2 to 4 mm fractions of soils contaminated by MSW ashes, which was in accordance with the prediction made based on the mineralogical and densimetric characterization. Moreover, as it can be seen, the concentration of Zn was significantly increased in the treated fraction of MSW1 and MSW3. Indeed, the quantity of Zn was concentrated in this fraction instead of in the mass of concentrate removed. This is explained by the fact that Zn can be incorporated to a light matrix, as the case of particle 5 in Table 3 ($Pb_aZn_bTi_cSi_dAl_eO_fCa_gCr_h$). Such phase is characterized by a low density (2.9–3.6 g/cm^3), which limit its separation by the gravimetric device. When compared with metal removal yields obtained by DMS, the low/moderate loss of efficiency in treating Cu, Pb, and Sn using the jig may have been caused by the

co-presence of carbonate phases, e.g., particle 8 in Table 3, characterized by a concentration criterion of 1.76. In such a case, separation is possible but difficult (USEPA, 1995). In addition, the presence of contaminants embedded in a significant volume of silica matrix, e.g., particle 6 in Table 3, which is characterized by a concentration criterion of 1.24–1.36, renders the gravimetric separation impossible (USEPA, 1995).

In the case of RM1, according to the mineralogical analysis of the 2–4 mm particles (Table 4), despite the fact that difficult separation of Cu and Zn was predicted (maximum mean density=3.6, concentration criterion=1.59), high removal yields were obtained (>65%). These removal yields were close to those predicted by DMS (R_M [Cu, Zn]>0.71).

Generally, for all soils, densimetric characterization was effective at predicting jig performance. However, the complexity of mechanisms involved during jig operation (i.e., differential acceleration, hindered settling, and interstitial trickling) (Wills, 2011), and the mineralogy of some contaminants, resulted in a low/moderate loss of jig performance compared to that predicted by both the mineralogical characterization and DMS.

3.4.1.1. Whole process efficiency

Tables 7, 8, 9, and 10 show the efficiency of the whole physical process proposed to treat MSW1, MSW2, MSW3, and MR1.

For MSW1 (Table 7), water washing coupled with magnetic treatment enhanced the removal of Zn from the coarse soil fraction (>4 mm) with moderate to high removal yields (51%–90%). The concentration of Cu was slightly reduced in the 4–12 mm fraction (removal=28%) whereas the concentration of Sn, known to be closely bound to Fe oxides, was significantly reduced (removal=80%). Attrition scrubbing followed by jigging, performed on the 2–4 mm soil fraction, lowered the concentrations of Pb and Sn, with removal yields higher than 68%. Furthermore, this procedure removed part of the Cu content (removal=48%). However, the concentration of Cu remained relatively high in the treated fraction. Attrition scrubbing of 0.25–1 mm and 1–2 mm fractions of MSW1 coupled with the action of the wet shaking table enabled high Pb and Sn removal (>54%). A moderate to high removal of Cu (33%–65%) was also observed for the 0.25–1 mm and 1–2 mm fractions of MSW1.

Table 8 shows that for MSW2, both water washing and permanent magnet separation achieved a significant decrease in the concentrations of Zn, Pb, and Sn from the >4 mm soil fraction of MSW2 (Pb removal >49%, Zn and Sn removals >75%). These treatments were also efficient in separating Cu from the >12 mm soil fraction. However, no effect was observed in extracting Cu from the 4–12 mm soil fraction. Attrition scrubbing of the 2–4 mm fraction of MSW2 followed by jigging led to an interesting decrease in the concentrations of Cu, Pb, and Sn (removals >62%), whereas up to 68% of Cu, Pb, and Sn were removed from the same fraction when using attrition scrubbing and the wet shaking table.

According to Table 9, both water washing and magnetic treatment lowered the concentration of Zn in the >4 mm fraction of MSW3, as was observed for MSW1 and MSW2 (removal >70.5%). Pb and Sn were efficiently removed from the >4 mm fraction with a removal yield higher than 82.3%. The concentration of Cu was significantly decreased in the >12 mm soil fraction (98.4%). However, the concentration of Cu remained high in the 4–12 mm soil fraction. Similarly to MSW1 and MSW2, attrition scrubbing coupled with jigging or wet shaking led to significant removal of Cu, Pb, and Sn from the 2–4 mm, 1–2 mm, and 0.25–1 mm fractions of MSW3 (removals >70.2%). Previous work has highlighted the difficulty of separating Cu from coarse fractions of soils contaminated with MSW ashes

when using low magnetic fields, probably because of the existence of diamagnetic elemental Cu (Mercier et al., 2002).

For MR1 (Table 10), water washing and magnetic separation were not efficient at separating Zn from the >4 mm fraction. However, substantial removal of Cu (>43%) was achieved, but the concentration of Cu remained quite high nevertheless. Indeed, Cu and Zn may be embedded in a diamagnetic silicate matrix, which prevents their separation from uncontaminated particles. Attrition scrubbing and jigging processes performed to treat the 2–4 mm soil fraction removed up to 75% of metallic contaminants. The concentrations of Cu and Zn were therefore highly reduced in the 2–4 mm soil fraction. For the 0.25–1 and 1–2 mm soil fractions, attrition scrubbing and wet shaking also achieved satisfactory Cu and Zn removal, ranging from 55 to 80%.

Overall, with respect to the physical treatment of the >0.25 mm fraction, the level of heavy metals in soils contaminated by MSW ashes was considerably reduced. The removal yields of Ba, Cu, Pb, Sn, and Zn varied from 50.8% to 64.7%, 42.1% to 71.9%, 56.9% to 80.1%, 66.7% to 83.4%, and 65.4% to 69.2%, respectively, depending on the level of inorganic pollution. The treated mass recovered from the >0.25 mm soil fraction ranged from 57.1% to 73.4%. This indicated the high efficiency of physical processes in concentrating metals in a small and acceptable volume of soil. For MR1, considering the >0.25 mm fraction, the removed mass of Cu and Zn varied from 57.6% to 65.5%. A satisfactorily treated mass was recovered from the >0.25 mm soil fraction, corresponding to 64.8% removal.

This work confirms the efficiency and broad applicability of physical processes in treating several types of heterogeneous contaminated soils when metals are potentially separable, as predicted based on densimetric and mineralogical characterization. For instance, Laporte-Saumure et al. (2010) reported Pb, Cu, and Zn removal yields higher than 66% when treating army shooting range backstop soil by jigging and wet shaking. Similarly, Jobin et al. (2016b) obtained up to 64% of Pb, Cu, and Sn removal when treating MSW ash contaminated soils by attrition scrubbing and gravimetric separation processes. Furthermore, Bisone et al. (2013) reported up to 80% removal of Cu and Zn when treating soils contaminated by metallurgical residues.

4. Conclusion

Inorganic contaminants were heterogeneously distributed in fractions of soils contaminated by MSW ashes and the soil contaminated by metallurgical residues. A specific treatment of each soil fraction was, consequently, needed. Mineralogical and densimetric characterization revealed the usefulness and limitations of using gravimetric processes, namely, the jig and the wet shaking table, to reduce the level of metals in polluted soils. When using the TBE separation, Cu, Pb, and Sn in the 0.25–1 mm, 1–2 mm, and 2–4 mm fractions of soils contaminated by MSW ashes, were highly concentrated in the heavy fraction. In the same way, during the TBE separation, Cu and Zn in the 0.25–1 mm, 1–2 mm, and 2–4 mm fractions of soil contaminated by metallurgical residues, were, too, highly concentrated in the heavy fraction. Satisfactory removals yields of these contaminants, when using gravimetric separation, were then predicted.

The mineralogical investigation of 2–4 mm, 1–2 mm and 0.25–1 mm soil fractions enabled the estimation of mean densities of particles and their corresponding concentration criterion to predict their fate under gravimetric forces. Contaminated particles derived from MSW ashes and metallurgical residues were therefore classified into three major groups. The first and the second groups consisted   of   to-

tally liberated contaminants and contaminants found bound to a heavy phase. Such contaminated particles were characterized by a mean density higher than $3.90\,g/cm^3$ and a concentration criterion higher than 1.76, allowing their efficient separation from uncontaminated particles by jigging and wet shaking. However, the third group was characterized by contaminants entrapped within a silica matrix or bounded to a silica matrix, calcium carbonate phase, or calcite phases. A loss of efficiency of gravimetric devices was therefore expected depending on the nature and volume occupied by the light phase for such contaminated particles and their distribution inside the soil sample.

As well as predicting the efficiency of gravimetric processes, TBE separation enabled the optimization of the jigging process while minimizing the number of assays. By comparing the contaminant mass removed using the jig and DMS the number of passes required through the device was determined. Approximately 3, 5, 10, and 20 passes were required to effectively treat the 2–4 mm fraction of MSW1, MSW2, MSW3, and MR1, respectively. The removal yields of Cu, Pb and Sn, from the 2–4 mm fraction of soils contaminated by MSW ashes, was moderately to highly close to that, obtained by the TBE separation (ranging from 25.3% to 70.8%). The removal yields of Cu and Zn were too close to that obtained by the TBE separation (ranging from 35.3% to 70.1%).

After exhaustive characterization of soil fractions, the global physical remediation process was established. Water washing coupled with the use of a permanent magnet (>4 mm), attrition scrubbing coupled with jigging (2–4 mm), and wet shaking (0.25–2 mm) successfully removed more than 50% of inorganic contaminants present in the >0.25 mm fraction of the studied soils. This indicates the usefulness and the broad applicability of physical remediation processes to remove separable metals from soil with different types and levels of inorganic pollution. However, further investigations are recommended concerning the treatment of coarse fractions of soils and for optimizing the attrition scrubbing processes.

Uncited references

ITRC (2011).

Acknowledgments

Appendix A. Supplementary material

Supplementary data to this article can be found online at https://doi.org/10.1016/j.wasman.2019.05.031.

References

Bisone, S., Mercier, G., Blais, J., 2013. Decontamination of metals and polycyclic aromatic hydrocarbons from slag-polluted soil. J. Environ. Technol. 34, 2633–2648. https://doi.org/10.1080/09593330.2013.781231.

Chandler, A., Eighmy, T., Hjelmar, O., Kosson, D., Sawell, S., Vehlow, J., Van der Sloot, H., Hartlén, J., 1997. Municipal Solid Waste Incinerator Residues, first ed. Elsevier Science, Amsterdam.

Chimenos, J., Segarra, M., Fernández, M., Espiell, F., 1999. Characterization of the bottom ash in municipal solid waste incinerator. J. Hazard. Mater. 64, 211–222. https://doi.org/10.1016/S0304-3894(98)00246-5.

Dermont, G., Bergeron, M., Mercier, G., Richer-Laflèche, M., 2008. Soil washing for metal removal: a review of physical/chemical technologies and field applications. J. Hazard. Mater. 152, 1–31. https://doi.org/10.1016/j.jhazmat.2007.10.043.

Dong, J., Chi, Y., Tang, Y., Ni, M., Nzihou, A., Weiss-Hortala, E., Huang, Q., 2015. Partitioning of heavy metals in municipal solid waste pyrolysis, gasification, and incineration. Energy Fuels 29, 7516–7525. https://doi.org/10.1021/acs.energyfuels.5b01918.

Forteza, R., Far, M., Seguí, C., Cerdá, V., 2004. Characterization of bottom ash in municipal solid waste incinerators for its use in road base. J. Waste Manage. 24, 899–909. https://doi.org/10.1016/j.wasman.2004.07.004.

FRTR, 2016. Ex situ physical/chemical treatment for soil, sediment, bedrock and sludge. https://frtr.gov/matrix2/section3/3_5.html/ (accessed 05.05.18).

GC, 2018. Lachine canal national historic site. The cradle of industrialization. https://www.pc.gc.ca/en/lhn-nhs/qc/canallachine/decouvrir discover/construction/industrialisation/ (accessed 07.05.18).

Horowitz, A., 1991. A Primer on Sediment-Trace Element Chemistry 2nd edition (Report 91–76). Unated States Geological Survey, Denver.

Iskandar, I., 2000. Environmental Restoration of Metals-Contaminated Soils, first ed. CRC Press, Boca Raton, London, New York, Washington.

ITRC, 2011. ITRC technical and regulatory guidance document: Development of performance specifications for solidification/stabilization (S/S-1, July 2011), The Interstate Technology & Regulatory Council - Solidification/Stabilization Team, Washington.

Jobin, P., Coudert, L., Taillard, V., Blais, J., Mercier, G., 2016. Remediation of inorganic contaminants and polycyclic aromatic hydrocarbons from soils polluted by municipal solid waste incineration residues. J. Environ. Technol. 37, 1983–1995. https://doi.org/10.1080/09593330.2015.1137636.

Jobin, P., Mercier, G., Blais, J., 2016. Magnetic and density characteristics of a heavily polluted soil with municipal solid waste incinerator residues: Significance for remediation strategies. Int.. J. Miner. Process. 149, 119–126. https://doi.org/10.1016/j.minpro.2016.02.010.

Jobin, P., Mercier, G., Blais, J., Taillard, V., 2015. Understanding the effect of attrition scrubbing on the efficiency of gravity separation of six inorganic contaminants. Water Air Soil Pollut. 226, 162. https://doi.org/10.1007/s11270-015-2422-6.

Kabata-Pendias, A., 2011. Trace Elements in Soils and Plants, fourth ed. CRC Press, Boca Raton.

Khalid, S., Shahid, M., Niazi, N., Murtaza, B., Bibi, I., Dumat, C., 2017. A comparison of technologies for remediation of heavy metal contaminated soils. J. Geochem. Explor. 182, 247–268. https://doi.org/10.1016/j.gexplo.2016.11.021.

Kowalski, P., Kasina, M., Michalik, M., 2017. Metallic elements occurrences in the municipal waste incineration bottom ash. Energy Procedia 125, 56–62. https://doi.org/10.1016/j.egypro.2017.08.060.

Laporte-Saumure, M., Martel, R., Mercier, G., 2010. Evaluation of physicochemical methods for treatment of Cu, Pb, Sb, and Zn in Canadian small arm firing ranges backstop soils. Water Air Soil Pollut. 213, 171–189. https://doi.org/10.1007/s11270-010-0376-2.

MDDELCC, 2017. Protection des sols et réhabilitation des terrains contaminés - Loi et règlements. Ministère du développement durable, de l'environnement et de la lutte contre les changements climatiques. http://www.mddelcc.gouv.qc.ca/sol/terrains/loi-reg.htm/ (accessed 04.12.17).

Mercier, G., Duchesne, J., Blackburn, D., 2001. Prediction of metal removal efficiency from contaminated soils by physical methods. J. Environ. Eng. 127, 348–358. https://doi.org/10.1061/(ASCE)0733-9372(2001) 127:4(348).

Mercier, G., Duchesne, J., Blackburn, D., 2002. Removal of metals from contaminated soils by mineral processing techniques followed by chemical leaching. J. Water Air Soil Pollut. 135, 105–130. https://doi.org/10.1023/A:1014738308043.

Min.Database, 2018. Mineralogy Database. http://webmineral.com/ (accessed 05.05.18).

Mouedhen, I., Coudert, L., Blais, J., Mercier, G., 2018. Study of factors involved in the gravimetric separation process to treat soil contaminated by municipal solid waste. J. Environ. Manage. 209, 23–36. https://doi.org/10.1016/j.jenvman.2017.12.020.

Piatak, N., Parsons, M., Seal, R., 2015. Characteristics and environmental aspects of slag: a review. J. Appl. Geochem. 57, 236–266. https://doi.org/10.1016/j.apgeochem.2014.04.009.

Piatak, N., Seal, R., 2012. Mineralogy and environmental geochemistry of historical iron slag, Hopewell Furnace National Historic Site, Pennsylvania, USA. J. Appl. Geochem. 27, 623–643. https://doi.org/10.1016/j.apgeochem.2011.12.011.

Piatak, N.M., Parsons, M.B., Seal, R.R., 2015. Characteristics and environmental aspects of slag: a review. J. Appl. Geochem. 57, 236–266. https://doi.org/10.1016/j.apgeochem.2014.04.009.

Ramachandra Rao, S., 2006. Chapter 8 - Metallurgical Slags, Dust and Fumes. In: Ramachandra Rao, S. (Ed.), Waste Management Series. Elsevier, Amsterdam, pp. 269–327.

Shen, H., Forssberg, E., 2003. An overview of recovery of metals from slags. J. Waste Manage. 23, 933–949. https://doi.org/10.1016/S0956-053X(02)00164-2.

Sungur, A., Soylak, M., Ozcan, H., 2019. Fractionation, source identification and risk assessments for heavy metals in soils near a small-scale industrial area (canakkale-Turkey). J. Soil Sediment Contam. 28, 213–227. https://doi.org/10.1080/15320383.2018.1564735.

USEPA, 1995. Contaminants and remedial options at selected metal-contaminated
    sites (EPA/540/R-95/512 July 1995), United States Environmental Protection
    Agency - Office of Research and Development, Washington.
Veetil, D., Mercier, G., Blais, J.F., Chartier, M., Tran, L., Taillard, V., 2014. Remedia-
    tion of contaminated dredged sediments using physical separation techniques. J.
    Soil Sediment Contam. 23, 932–953. https://doi.org/10.1080/15320383.2014.
    896860.

Wei, Y., Shimaoka, T., Saffarzadeh, A., Takahashi, F., 2011. Mineralogical characteri-
    zation of municipal solid waste incineration bottom ash with an emphasis on heavy
    metal-bearing phases. J. Hazard. Mater. 187, 534–543. https://doi.org/10.1016/j.
    jhazmat.2011.01.070.
Wills, B., 2011. Wills' Mineral Processing Technology: An Introduction to the Practi-
    cal Aspects of Ore Treatment and Mineral Recovery, seventh ed. Butter-
    worth-Heinemann, Amsterdam.